nature immunology

© 2003 Nature Publishing Group http://www.nature.com/natureimmunology

Dynamics of CD8+ T cell priming by dendritic cells in intact lymph nodes

Philippe Bousso & Ellen Robey

The cellular dynamics underlying activation of CD8+ T cells by dendritic cells (DCs) in the lymph node are not known. Here we have tracked the behavior of T cells and DCs by subjecting intact lymph nodes to real-time two-photon microscopy. We show that DCs scan at least 500 different T cells per hour in the absence of antigen. Antigen-bearing DCs are highly efficient in recruiting peptide-specific T cells and can engage more than ten T cells simultaneously. The duration of these interactions is of the order of hours, not minutes. The overall avidity of the interaction influences the probability that T cells will be stably captured by DCs, providing a possible basis for T cell competition. Taken together, our results identify the cellular behaviors that promote an efficient CD8+ T cell response in the lymph node.

Most T cell responses are initiated in the paracortical region of the lymph node, where antigen-bearing DCs that have migrated from inflamed tissues activate antigen-specific T lymphocytes. Before immunization, antigen-specific $CD8^+$ T cells are present at very low frequency (typically 1 in 10^5–10^6 T cells) in the T cell repertoire. Therefore, antigen-bearing DCs must sample a large fraction of the T cell pool to physically engage one or several antigen-specific T cells. Subsequently, antigen recognition can lead to T cell activation and clonal expansion.

Studies using fixed lymph node sections have shed light on antigen recognition *in vivo*[1–4]. For example, $CD4^+$ T cells contacting antigen-pulsed DCs have been visualized[1], and interactions between $CD8^+$ T cells and DCs infected by a recombinant vaccinia virus have been observed[3]. Although such studies have confirmed the important role of antigen presentation by DCs in lymphoid organs, they provide only a static picture of antigen-driven cellular interactions and cannot address additional important issues such as cellular migration or contact dynamics. Imaging studies of cell suspensions have shown that antigen recognition can induce T cells to stop, form and maintain an ordered immunological synapse, and engage in a long-lasting interaction (>1 h) with the antigen-presenting cell (APC)[5–9]. Other reports have shown that T cell activation can occur as the result of multiple, transient interactions with APCs[10,11].

To understand better the mode of T cell activation *in vivo*, it is essential to analyze T cell and DC behavior in their native environment of the lymph node. We and others have shown that two-photon laser scanning microscopy (TPLSM) can track individual lymphocytes located deep within three-dimensional lymphoid tissues[12,13]. Two studies have analyzed $CD4^+$ T cell responses in intact lymph nodes. In the first, TPLSM was used to image paracortical $CD4^+$ T cell behavior in the lymph node[13]. T cells were found to be highly motile before immunization. After antigen challenge, clusters of T cells were observed, some of which were stable and some of which showed swarming behavior. Although APCs were not imaged in those experiments, the observation that T cells could remain highly motile while in contact with APCs suggested that the contacts might be relatively short-lived. In the second study, confocal microscopy was used to visualize both $CD4^+$ T cells and bone marrow–derived DCs[14]. T cells were found to be generally nonmotile before and during antigen stimulation, and stable, long-lived contacts with DCs were observed.

In addition to the above uncertainties regarding T cell motility and the stability of T cell–APC contacts, there is very little information available on the behavior of $CD8^+$ T cells and DCs in lymphoid organs. Here we address these issues by using TPLSM to track in real-time the physical interactions between fluorescently labeled $CD8^+$ T cells and DCs in an intact lymph node. We show that the high motility of T cells, as well as the membrane dynamics of DCs, facilitates an extremely efficient scanning of the T cell repertoire. We also show that antigen recognition results in long-lasting contacts between individual $CD8^+$ T cells and DCs. Last, we examine how the pattern of T cell–DC contacts changes with the number of APCs and the overall T cell avidity.

RESULTS

T cell and DC motility in the lymph node

To analyze the pattern of T cell and DC migration in the lymph node, splenic DCs labeled with seminapthorhodafluor (SNARF) were injected subcutaneously and polyclonal T cells labeled with carboxyfluorescein diacetate succinimidyl ester (CFSE) were injected intravenously into naive C57BL/6 (B6) mice. After 20 h, intact draining lymph nodes were isolated and subjected to real-time TPLSM imaging at 37 °C, while being perfused with medium bubbled with 95% oxygen. Dye-labeled T cells and DCs were detected up to 200 m below the tissue surface in the paracortical region of the lymph node.

Department of Molecular and Cell Biology, University of California, Berkeley, California 94720, USA. Correspondence should be addressed to P.B. (bousso@pasteur.fr).

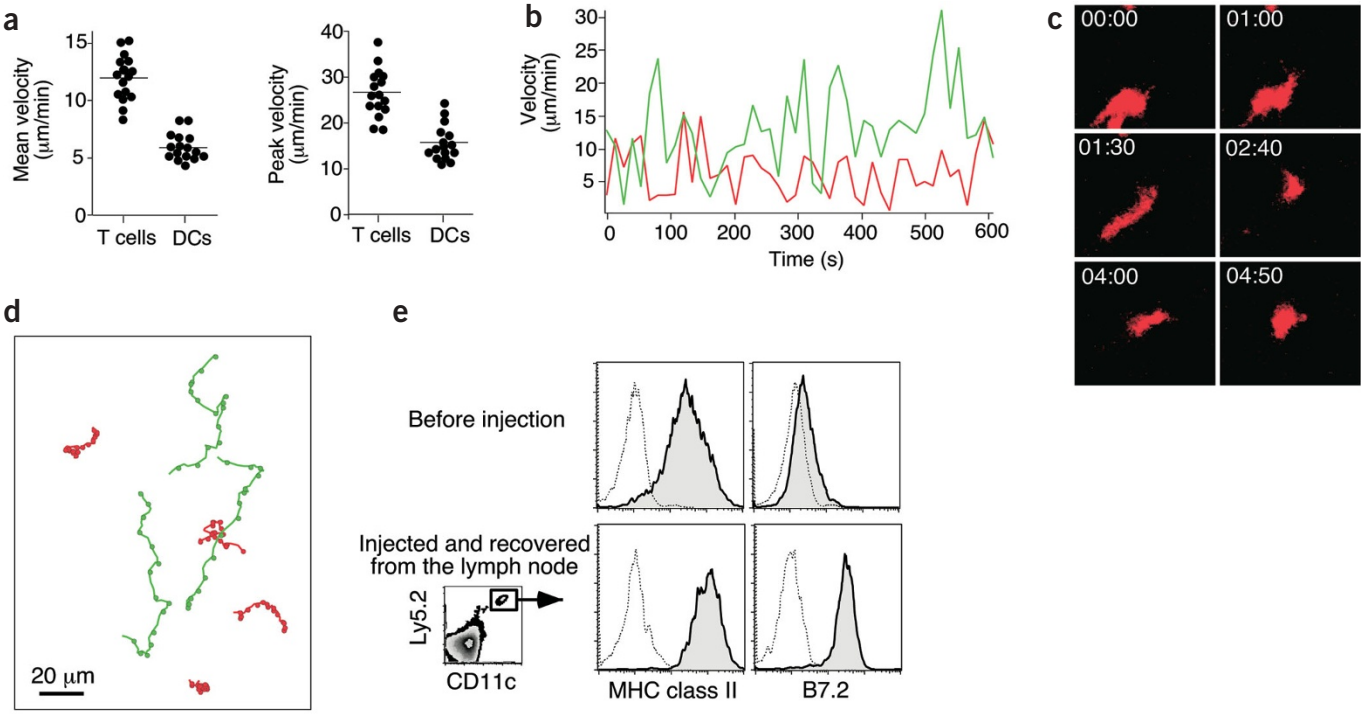

Figure 1 Motility of T cells and DCs in the lymph node. Intact lymph nodes containing CFSE-labeled polyclonal T cells and SNARF-labeled DCs were visualized by real-time two-photon imaging. Individual cells were imaged every 10 s for about 10 min. (**a**) Mean velocity of 16 individual T cells and DCs (left) and peak velocity achieved during the period of imaging (right). (**b**) Velocity of a representative T cell (green) and a DC (red) plotted over time. (**c**) Frames from a time-lapse movie showing the migration and extensive shape changes undergone by a representative DC. The time (min:s) that each frame was taken is indicated. (**d**) Representative trajectories of three T cells (green) and four DCs (red). Dots indicate the position of the cell at 40-s intervals. (**e**) Injected DCs recovered from the draining lymph node show the hallmarks of mature DCs. Splenic DCs were isolated from B6 mice (Ly5.2) and injected subcutaneously into B6 Ly.5.1 mice. Flow cytometry was used to assess the expression of MHC class II and B7.2 on DCs before injection (top) and on cells from the draining lymph node (after collagenase treatment) obtained 20 h after injection (bottom). All data are gated on $Ly5.2^+CD11c^+$ cells. Dotted lines represent staining with an appropriate isotype control antibody.

© 2003 Nature Publishing Group http://www.nature.com/natureimmunology

In the lymph nodes of young mice, a high density of dye-labeled T cells was usually seen about 80–100 m below the capsule surface. We confirmed that these regions corresponded to T cell areas and were usually located below B cell follicles by imaging lymph nodes containing dye-labeled T cells and B cells (data not shown). T cells were highly motile, with an average velocity of 11.9 ± 1.9 m/min (mean ± s.d.) and peak velocities of 26.5 ± 4.9 m/min (**Fig. 1a**,**b** and **Supplementary Video 1** online). DCs were also motile but to a lesser extent, with an average velocity of 5.9 ± 1.0 m/min and peak velocities of 15.6 ± 3.6 m/min (**Fig. 1a**,**b** and **Supplementary Video 1** online). DC velocity was influenced by cell migration and shape changes that resulted in a rapid movement of the center of mass of the cell (**Fig. 1c**). Both T cells and DCs showed relatively random trajectories (**Fig. 1d**).

To determine the phenotype of the DCs imaged, we injected splenic DCs isolated from B6 Ly5.2 mice into congenic B6 Ly5.1 recipients and recovered the draining lymph node after 20 h. Flow cytometry analysis showed that purified DCs that had migrated into the lymph node had the hallmarks of mature DCs, including high expression of major histocompatibility complex (MHC) class II molecules and B7.2 (**Fig. 1e**). Of note, MHC class II and B7.2 expression was higher than in these cells than in the DCs before injection (**Fig. 1e**). This phenotype change could be due to the DC isolation procedure and/or to the migration process.

We determined by flow cytometry that 10^3–10^4 transferred DCs migrated into the draining lymph node in our experiments. These numbers are in the physiological range, because similar numbers of DCs migrate into the lymph node draining an inflamed tissue[15,16]. Finally, the percentage of $CD8\alpha^+$ DCs out of $CD11c^+$ DCs was 20% and 30% before injection and after recovery in the draining lymph node, respectively.

Sampling of T cells by individual DCs

The high velocities reached by T lymphocytes and the rapid shape changes of DCs enabled each DC to contact several labeled T cells over a short period of time (**Figs. 2a**,**b** and **Supplementary Videos 1** and **2** online). To quantify the number of labeled T cells that came in contact (usually for a very short time) with each DC, we recorded images from several optical planes containing the DCs over time. The recording period varied for each DC, depending on the time that the DCs remained in the imaged planes. The proportion of CFSE-labeled T cells out of the total T cell population (typically 2%) was measured by flow cytometry and used to estimate the total number of T cells (labeled and unlabeled) that contacted the DCs over the imaging period (**Fig. 2c**).

We calculated that 7.3 new T cells (95% confidence interval, 4.4–10.0 T cells) came into close contact with each individual DC per minute. Extrapolation of these measurements indicates that each DC can contact about 500 different T cells in an hour (95% confidence interval, 317–619 T cells). This number might be an underestimate, however, as we may not be able to visualize T cells contacting very thin DC processes. We conclude from these results that the pattern of cell motility in the lymph node supports a very efficient scanning of the T cell repertoire by individual DCs.

© 2003 Nature Publishing Group http://www.nature.com/natureimmunology

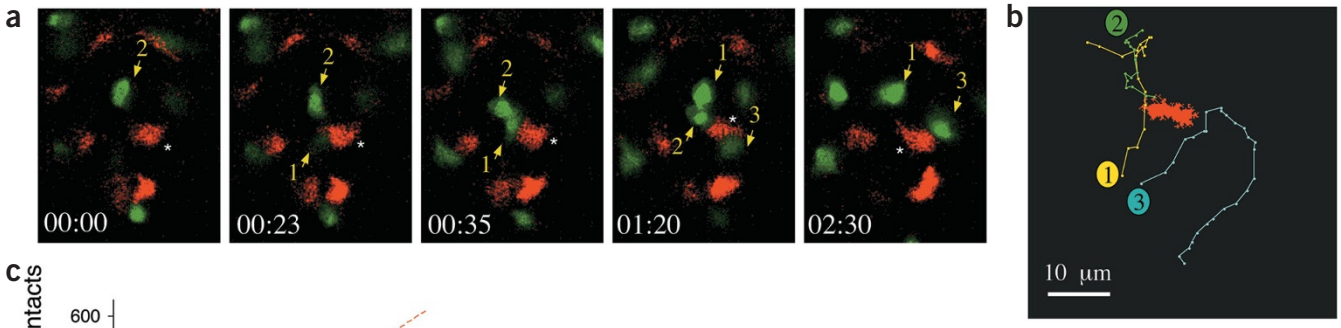

Figure 2 T cell migration promotes very efficient scanning of the T cell repertoire by an individual DC. (**a**) Several different polyclonal T cells (green) come into close proximity of an individual DC (red, marked by an asterisk) over a short period of time. Arrows indicate the position of three T cells at different time points. (**b**) Trajectories of the T cells shown in **a**. The average position of the DCs is shown in red. (**c**) Estimated T cell contacts. Several planes encompassing individual DCs were imaged over time and the number of labeled T cells that came into close proximity of the DCs was recorded. The total number of T cells (endogenous and CFSE-labeled) scanned by the DCs was estimated by measuring by flow cytometry the percentage of CFSE-labeled T cells out of the total $CD3^+$ T cells in lymph nodes from the same mouse. Results are plotted as a function of imaging time. A linear regression was done (correlation coefficient, $r = 0.7$), and the best-fit line (unbroken red) and curves delineating the 95% confidence interval (broken red) are shown. The graph indicates that about 500 T cells are scanned by one DC in 1 h.

$CD8^+$ T cell behavior on antigen recognition

To analyze $CD8^+$ T cell priming by DCs, we used naive $CD8^+$ T cells from P14 peptide–specific T cell antigen receptor (TCR) transgenic *Rag2*$^{-/-}$ mice (hereafter referred to as P14 TCR T cells). These T lymphocytes recognize the gp33 epitope from the lymphocytic choriomeningitis virus[17]. Naive B6 mice were injected subcutaneously with either unpulsed or gp33-pulsed DCs and intravenously with CFSE-labeled P14 TCR T cells. This experimental procedure induced a very efficient immune response, as shown by the large extent of P14 TCR T cell proliferation observed 3 d after injecting DCs pulsed with 1 M of gp33 peptide (**Fig. 3a**). A similar pattern of proliferation was observed for peptide concentrations ranging from 1 nM to 1 M (data not shown). Cell proliferation started to decrease for peptide concentrations below 300 pM. Of note, the frequency of divided cells and the number of cell divisions undergone were substantially lower when DCs were pulsed with a low concentration (30 pM) of peptide (**Fig. 3a**).

Twenty hours after injection, real-time imaging experiments of labeled T cells showed that more than 50% of the P14 TCR T cells were engaged by DCs pulsed with 1 M gp33 peptide (**Fig. 3b**). These interactions were driven mainly by antigen recognition, because most P14 TCR T cells located in a lymph node containing unpulsed DCs were actively crawling and only a few were observed to interact with the injected DCs (**Fig. 3b**). A substantial fraction of P14 TCR T cells (38%) remained freely crawling in lymph node containing peptide-pulsed DCs (**Fig. 3b**). This may reflect heterogeneity in the timing of when individual T cells enter the lymph node after injection. In particular, T cells that arrived in the lymph node just before removal of the lymph node for imaging would have less time to migrate throughout the lymph node and therefore would have a lower probability of encountering a peptide-pulsed DCs than those that arrived earlier. In addition, some P14 TCR T cells might have already interacted with a peptide-pulsed DCs and reacquired a motile behavior at the time of imaging.

To gain insight into the dynamics and the duration of the cellular interactions, individual T cell–DC contacts were imaged over time (**Fig. 4** and **Supplementary Video 3** online). Because of the degree of DC motility, T cell–DC clusters moved out of the imaged planes over time, making it technically difficult to follow individual interactions for extended periods. A total of 42 T cell–DC interactions were tracked for an average duration of 11 min (range 4–26 min), representing a cumulative imaging time of 7.5 h.

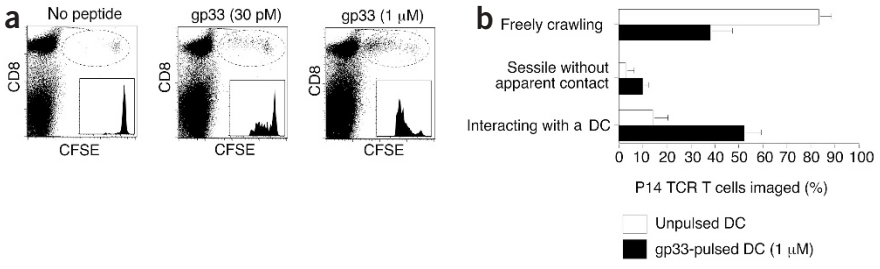

Figure 3 Changes in $CD8^+$ T cell behavior on antigen recognition. (**a**) Three days after the injection of DCs (unpulsed or pulsed with the indicated concentration of gp33 peptide) and CFSE-labeled P14 TCR T cells, cells from the draining lymph node were stained with a monoclonal antibody to CD8. Insets show the dilution of the CFSE fluorescence on gated CFSE-positive cells. Results are representative of four lymph nodes analyzed for each peptide concentration. (**b**) Behavior of CFSE-labeled P14 TCR T cells located in lymph nodes containing SNARF-labeled DCs pulsed with 1 M gp33 peptide or left unpulsed. At 20 h after injection, several locations in the T cell area of the draining inguinal lymph node were imaged over time. Each P14 TCR T cell was categorized as freely crawling, as sessile with no apparent contact with a DC, or as interacting with a DC. Any contact between a T cell and a DC that lasted for at least 2 min was defined as an interaction. Results are the mean ± s.d. of measurements derived from four (peptide-pulsed DCs) and three (unpulsed DCs) time-lapse movies, representing 81 and 59 T cells, respectively. Movies were recorded ~100 m below the lymph node surface. Results are representative of two independent experiments.

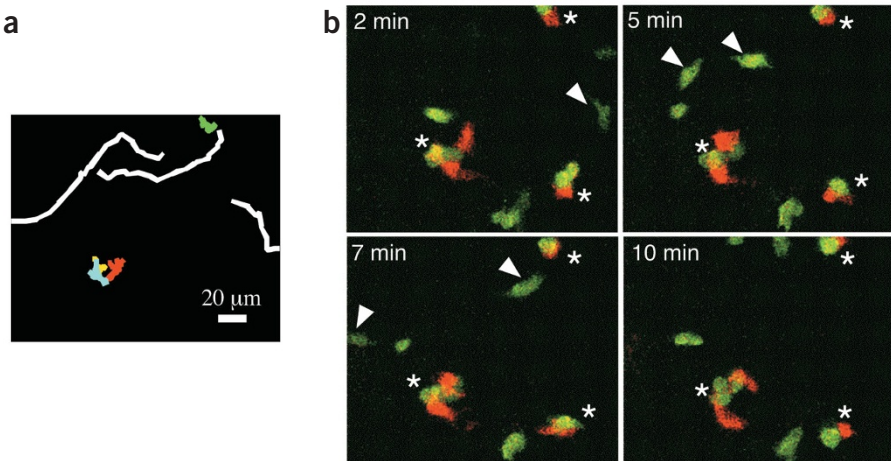

Figure 4 Priming of CD8$^+$ T cells by DCs occurs as long-lasting interactions. Real-time imaging of cellular interactions between P14 TCR T cells (green) and DCs pulsed with 1 M of gp33 peptide (red). Data are derived from a time-lapse movie (**Supplementary Video 3** online). (**a**) Trajectories of four P14 TCR T cells (yellow, red, green and cyan) that were engaged with DCs and three P14 TCR T cells that were freely crawling (white). Cells were imaged every 17 s for 12 min. (**b**) Time frame images showing T cells engaged with antigen-presenting DCs (marked by asterisks) and freely crawling T cells (arrows). The time relative to the beginning of the imaging experiment is indicated. All P14 TCR T cells that were engaged with DCs at the beginning of the experiment maintained contact for the whole duration of imaging.

In all cases (42/42), the contact between the T cell and the DCs was maintained for the whole period of imaging (**Fig. 4** and **Supplementary Video 3** online). If the mean duration of the T cell–DC contact were of the order of minutes, we would have observed a number of contact terminations during which the T cell detached from the DC. Because we did not, we conclude that the average duration of T cell–DC contacts on antigen recognition is of the order of hours, not minutes. The T cell–DC contacts, although long lasting, were not necessarily completely static. In some cases, slow crawling of the T cells on the DC surface and passive movement of the T cell owing to shape changes of the DCs were observed (**Fig. 4** and **Supplementary Video 3**).

Importance of DC numbers

To establish how the pattern of T cell–DC interactions changes when the density of DC varies, we imaged lymph nodes from mice injected with different numbers of DCs. When 2 10^6 DCs pulsed with 1 M of gp33 peptide were injected, we found that 1.8 ± 1.1 (mean ± s.d.) P14 TCR T cells interacted with each DC (**Fig. 5a**). Injection of only 5 10^5 DCs resulted in a substantial decrease in DC density in the paracortex and in a marked increase in cluster size, which comprised 6.1 ± 3.1 P14 TCR T cells per DC (**Fig. 5a**). In a few cases (16% of total DCs), DCs interacted simultaneously with more than ten P14 T cells. Three-dimensional reconstruction images showed that the surface area of these DCs was virtually saturated with P14 T cells (**Fig. 5b**,**c**).

These results underscore the efficiency of T cell recruitment by antigen-presenting DCs and indicate that, in this system, the limiting factor for the number of T cells engaged by a single DC is its surface area. Real-time imaging showed that most of the interactions in these large clusters were maintained over time (**Fig. 5d** and **Supplementary Video 4** online). This indicates that newly arrived T cells may have limited opportunity to interact with DCs under these conditions.

Effect of antigen density

The overall reduced extent of T cell proliferation (**Fig. 3b**) observed with a low concentration (30 pM) of peptide might be due to a

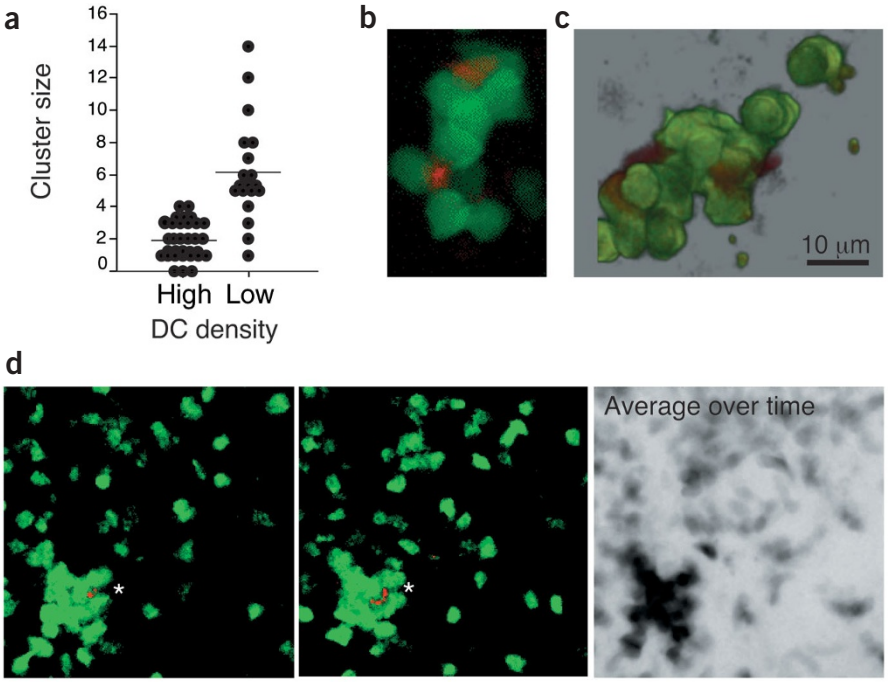

Figure 5 Impact of DC density on T cell–DC contacts. (**a**) Extent of T cell clustering as a function of the DC density in the lymph node. DC density in the T cell areas was experimentally modulated by injecting either 2 10^6 (high density) or 5 10^5 (low density) DCs pulsed with 1 M gp33 peptide. At 20 h, *z*-stacks of images were acquired in the T cell areas and used to count the number of P14 TCR T cells contacting each imaged DC. Each dot represents the cluster size around an individual DC. (**b**) A low density of DCs results in the formation of large clusters of T cells. Shown is a maximum intensity projection of a *z*-stack of images encompassing a cluster of T cells (green) around an individual DC (red). (**c**) Three-dimensional volume rendering obtained from a *z*-stack of images acquired 1 m apart shows that the surface of a DC can be saturated by contacting P14 TCR T cells. (**d**) Relative stability of the P14 TCR T cells engaged in large clusters. Two time frames imaged 4 min apart show a large cluster of T cells (asterisk) formed around an individual DC (left, middle). The CFSE signal from 50 time frames imaged over a 10-min period was averaged (right). P14 TCR cells whose positions remain relatively unchanged during this imaging period appear as dark cells.

© 2003 Nature Publishing Group http://www.nature.com/natureimmunology

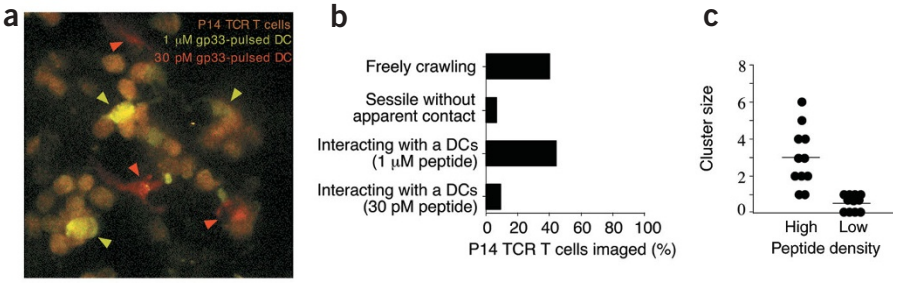

Figure 6 Low-avidity interactions result in inefficient recruitment of peptide-specific T cells by antigen-bearing DCs. After being pulsed with 1 M or 30 pM gp33 peptide, DCs were labeled with CFSE or SNARF, respectively, and mixed at a 1:1 ratio (1 10^6 DCs for each peptide concentration). P14 TCR T cells were simultaneously labeled with both dyes. (**a**) Maximum intensity projection of a *z*-stack of images showing P14 TCR T cells (orange), DCs with high densities of peptide (yellow-green, marked by green arrows) and DCs with low densities of peptide (red, marked by red arrows). (**b**) The behavior of 75 individual P14 TCR T cells was recorded and categorized as in **Fig. 3b**. Data are derived from one representative time-lapse movie out of five. (**c**) The cluster size around 22 individual DCs with either low or high peptide densities was estimated as in **Fig. 5**.

© 2003 Nature Publishing Group http://www.nature.com/natureimmunology

lower probability of cellular engagement with antigen-bearing DCs. Alternatively, cellular engagement might occur efficiently but subsequent signals or activation steps could be suboptimal. To investigate these possibilities, we compared the behavior of P14 TCR T cells in a lymph node containing both DCs pulsed with 1 M of gp33 peptide and DCs pulsed with 30 pM of gp33 peptide. These peptide concentrations consistently resulted in measurable differences in the extent of T cell proliferation, indicating that DCs pulsed with these peptide concentrations have differing peptide densities on their surface. DCs with high and low peptide densities were labeled with CFSE and SNARF, respectively, and the P14 TCR T cells were simultaneously labeled with both dyes. This experimental strategy enabled us to distinguish these three different populations of cells.

The binding of P14 TCR T cells to DCs bearing low densities of peptide was very inefficient as compared with binding to DCs bearing high densities of peptide (**Fig. 6a** and **Supplementary Video 5** online). Whereas 44% of the imaged P14 TCR T cells interacted with a DC that had been pulsed with the high peptide concentration, only 9% contacted a DC pulsed with the low peptide concentration (**Fig. 6b**). In addition, the average cluster size around DCs was 3 and 0.6 T cells for the high and low peptide densities, respectively (**Fig. 6c**).

As expected, virtually all contacts observed between P14 TCR T cells and DCs bearing high peptide densities were maintained during imaging periods of about 20 min (**Supplementary Video 6** online). Of the few contacts between P14 TCR T cells and a DC with a low peptide density, some were also maintained. Other contacts detached rapidly, similar to contacts between P14 TCR T cells and unpulsed DCs. We conclude from these results that the overall T cell avidity (modulated here by varying the antigen density on a DC) has a considerable impact on the probability that a T cell will form a long-lasting interaction with an antigen-bearing DC. Specifically, the probability for a P14 TCR T cell to be stably recruited by an antigen-bearing DC increases as the antigen density increases.

DISCUSSION

We have used TPLSM to examine the cellular dynamics of $CD8^+$ T cells and DCs in the lymph node before and during antigen recognition. In the absence of immunization, most polyclonal or P14 TCR $CD8^+$ T cells were actively crawling in the paracortex. The DCs also showed some degree of motility, as well as extensive and rapid shape changes.

Our results on T cell velocities are in agreement with a study by Miller *et al.*[13] but differ from the observation of Stoll *et al.*[14] that T cells are mostly nonmotile before immunization. This discrepancy may result from differences in the oxygen concentration of the samples. Although the isolation of intact lymph nodes preserves their cellular structure, it disrupts normal blood flow and innervation, which might alter the physiology of the sample. A potential concern is oxygen deprivation to the tissue. In both our study and that of Miller *et al.*[13], samples were perfused with medium that was bubbled with 95% oxygen to minimize this problem. Although it is possible that the nonphysiological oxygen concentration might have affected our results, a study of T cell migration in lymph nodes of live anesthetized mice found very similar velocities and behavior[18] to those observed with isolated lymph nodes in the presence of a high concentration (95%) of oxygen. This suggests that, although isolated lymph nodes do not recapitulate every aspect of the *in vivo* environment, they provide a faithful reflection of many aspects of cellular behavior under appropriate experimental conditions.

That even a small number of antigen-bearing APCs can detect the few available antigen-specific T cells and initiate an immune response has been puzzling. For example, no more than 80 APCs surrounded by clusters of antigen-specific T cells were detected in a lymph node of a mouse infected by a recombinant vaccinia virus[3]. Our results provide, in part, an explanation for this puzzle. The large surface area and irregular shape of DCs enable them to contact multiple T cells at a given time point. Another explanation may lie in the observation that both the pattern of T cell motility in lymph nodes and the rapid shape changes undergone by DCs promote numerous potential T cell–DC contacts. We estimated that each DC can potentially scan as many as 500 different T cells in an hour. Our observations suggest that as few as 200 DCs would be enough to detect a naive peptide-specific T cell present at a frequency of 1 in 10^5 cells in an hour. Such an efficient scanning of the T cell pool by DCs probably helps to ensure that, during localized infections, even a few DCs can initiate an antigen-specific T cell response.

Consistent with the large sampling of T cells by DCs before immunization, we found that recruitment of peptide-specific T cells by antigen-bearing DCs was highly efficient, because 1 d after injection more than half of the resident P14 TCR T cells were interacting with a peptide-pulsed DC. In this respect, we observed that fewer APCs could be compensated by the recruitment of more T cells by each individual DC. Our results show that, provided enough antigen is presented at the cell surface, there is no limit for the number of individual T cells that a DC can engage simultaneously other than that imposed by its surface area.

© 2003 Nature Publishing Group http://www.nature.com/natureimmunology

Previous studies have supported the idea that T cells can compete for access to the APCs[19,20]. Our findings—that under some conditions the surface of DCs can be 'saturated' with T cells for an extended duration—provide a possible physical basis for cell competition during an immune response in which the ratio of responding T cells to antigen-bearing APCs is high. Imaging experiments using two T cell populations with differing TCR affinities and/or peptide specificities should help to determine whether particular T cells can be physically excluded from the APC by others.

Our results indicate that an additional mechanism drives T cell competition during immune responses: that is, the probability of a T cell engaging an antigen-bearing DC is greatly influenced by the overall avidity of the interaction. In our study, T cell avidity was modulated by varying the peptide density at the surface of the DC. During a polyclonal T cell response, other parameters such as TCR affinity shape the overall T cell avidity. Our results support the idea that high-avidity T cells have a higher probability of being engaged by an antigen-bearing DC and therefore will be activated and start to proliferate before low-avidity T cells. This model is consistent with our observation that 3 d after DC injection the number of cell divisions undergone by P14 TCR T cells increased with the overall avidity of T cell–DC interactions. Such a mechanism might be involved in the selection for high-avidity T cells observed in several immune responses *in vivo*[21–24].

It should be noted that the APC population used in this study is likely to comprise several subtypes of DC[25]. Notably, virtually all DCs found to migrate to the draining lymph node after subcutaneous injection showed a mature phenotype, with high expression of MHC class II and B7.2 molecules. This phenotype was observed for both peptide-pulsed and unpulsed DCs, and whether or not P14 TCR T cells were present (data not shown). Thus, the interactions analyzed here pertain to contacts between mature DCs and naive $CD8^+$ T cells.

The stability of cellular contacts that occur during peptide-MHC recognition by T cells remains controversial. We previously observed that MHC recognition by developing T cells undergoing positive selection can occur as both stable and dynamic contacts with thymic stromal cells[12]. With respect to mature T cells, little is known about the behavior of $CD8^+$ T cells in lymphoid tissues, and studies aimed at analyzing $CD4^+$ T cells in physiological environments have reported conflicting results. For example, peptide-specific $CD4^+$ T cells in a collagen matrix were found to be activated as the result of multiple dynamic contacts with DCs, each of them lasting no longer than 6–12 min (ref. 11). One study of $CD4^+$ T cells in the lymph node has reported static contacts with antigen-bearing DCs[14], whereas another has reported that antigen-specific $CD4^+$ T cells form both stable and swarming clusters on immunization[13]. Because of the high density of T cells within swarms and the inability to visualize the APC, it was not clear from the latter study whether swarming T cells rapidly detached from the APC.

Because we visualized the T cell and the APC simultaneously, we could track any potential contact termination throughout the duration of imaging. As a general rule, T cell–DC contacts were maintained during imaging periods (up to ~30 min), even when the interactions did not seem to be completely static owing to either slow T cell crawling onto the surface of the DC or passive movement of the T cell caused by rapid shape changes of the DC. Thus, encounters between naive $CD8^+$ T cells and DCs bearing an optimal density of antigen result in stable, monogamous contacts. These results do not preclude a role for transient, promiscuous T cell–APC contacts in other contexts.

In summary, we have shown that the behavior of T cells and DCs in the lymph node promotes a very efficient scanning and recruitment of peptide-specific $CD8^+$ T cells by DCs. The formation of T cell–DC interactions is crucially dependent on T cell avidity. Notably, our results support the idea that $CD8^+$ T cell activation in the lymph node under optimal conditions of antigen presentation occurs as the result of a long-lasting interaction with a DC, rather than multiple short T cell–DC contacts. Static imaging has provided evidence that spatial molecular reorganization occurs at the T cell–APC contact *in vivo*[14,26,27]. TPLSM imaging of T cells expressing fluorescently tagged proteins should help to unravel the topology and the dynamics of the molecular reorganization occurring at the T cell–DC interface in living lymphoid organs.

METHODS

Mice. We purchased C57BL/6 mice from Jackson Laboratories and P14 TCR *Rag2*$^{-/-}$ mice from Taconic. All mice were maintained in our animal facility and experiments were done in compliance with the University of California Berkeley Animal Care and Use Committee.

Peptide and antibodies. The gp33 peptide (KAVYNFATM) has been described and was a gift of D. Raulet (University of California, Berkeley). Phycoerythrin (PE)-Cy5-conjugated anti-CD8 and purified anti-CD16/32 were purchased from eBioscience. We obtained biotinylated anti-Ly5.2, PE-conjugated anti-CD11c, fluorescein isothiocyanate (FITC)-conjugated anti–I-A^b and FITC-conjugated anti-B7.2 from PharMingen.

Cell preparation. Polyclonal T cells were isolated from the lymph nodes of B6 mice using a T cell enrichment column (R&D Systems). The cell purity was >96%. We isolated P14 TCR T cells from the spleen and lymph nodes of P14 TCR *Rag2*$^{-/-}$ mice. For splenic DC isolation, spleens from B6 mice were incubated in RPMI medium containing 1 mg/ml of collagenase D (Roche) and 50 g/ml of DNase I (Roche), injected with 1 ml of the same medium, cut into small fragments and incubated at 37 °C for 45 min. Cells were then dissociated and incubated with anti-CD11c–conjugated microbeads (Miltenyi Biotech) in the presence of 25 g/ml of anti-CD16/32. We isolated $CD11c^+$ cells by two consecutive rounds of selection using an AutoMacs system (Miltenyi Biotech). This procedure yielded a cell population containing >90% DCs. In some experiments, DCs were pulsed with the indicated concentration of gp33 peptide for 1 h at room temperature and then extensively washed. T cells were labeled with 10 M CFSE (Molecular Probes) for 15 min at 37 °C and DCs were labeled with 5 M SNARF (Molecular Probes) for 10 min at 37 °C. T cells were injected intravenously 3–4 h after the subcutaneous injection of DCs taken from B6 mice aged ~3 weeks. We injected the DCs at two sites under the skin above the inguinal lymph node. Young recipient mice were used to minimize the depth required for detecting the T cell areas in the lymph nodes.

Two-photon microscopy. Draining inguinal lymph nodes were carefully dissected, glued onto a coverslip and placed into a 35-mm culture dish containing Dulbecco's modified Eagle's medium (DMEM) without phenol red. The dish was inserted in a heated ring and the sample was perfused with warmed medium bubbled with a gas mixture containing 95% O_2 and 5% CO_2. The temperature close to the sample was monitored and maintained between 36 °C and 37 °C. We used an upright Zeiss NLO 510 microscope for imaging. Excitation light was provided by a MaiTai femtosecond tunable Ti:sapphire laser (Spectra-Physics) and focused onto the specimen using an achroplan IR 40 /0.8 dipping objective (Zeiss). CFSE and SNARF emissions were separated with either a 545-nm or a 560-nm dichroic filter (Chroma). Emission was collected using either two internal photon multiplier tubes or two non-descanned detectors (Zeiss). For time-lapse imaging, 3–4 planes spaced 5 m apart and located at least 100 m below the lymph node capsule were imaged typically every 10–20 s. When counting T cell–DC interactions, we ensured that signals from the T cell and DCs were directly in contact in the same *z* plane. Data were processed further using National Institutes of Health (NIH) Image and Igor Pro software (WaveMetrics). Three-dimensional volume rendering was done using Imaris software (Bitplane AG).

Note: Supplementary information is available on the Nature Immunology website.

ACKNOWLEDGMENTS

We thank H. Aaron for assistance with microscopy, N. Bhakta for advice on velocity measurements and N. Fernandez, W. Sha, D. Raulet and the members of the Robey laboratory for comments on the manuscript. This work was supported by NIH grants AI32985 and AI42033. P.B. is supported by the Cancer Research Institute.

COMPETING INTERESTS STATEMENT

The authors declare that they have no competing financial interests.

Received 28 February; accepted 10 April 2003
Published online 5 May 2003; doi:10.1038/ni928

1. Ingulli, E., Mondino, A., Khoruts, A. & Jenkins, M.K. *In vivo* detection of dendritic cell antigen presentation to CD4+ T cells. *J. Exp. Med.* **185**, 2133–2141 (1997).
2. Schaefer, B.C., Schaefer, M.L., Kappler, J.W., Marrack, P. & Kedl, R.M. Observation of antigen-dependent CD8+ T-cell/dendritic cell interactions *in vivo*. *Cell Immunol.* **214**, 110–122 (2001).
3. Norbury, C.C., Malide, D., Gibbs, J.S., Bennink, J.R. & Yewdell, J.W. Visualizing priming of virus-specific CD8+ T cells by infected dendritic cells *in vivo*. *Nat. Immunol.* **3**, 265–271 (2002).
4. Ingulli, E., Ulman, D.R., Lucido, M.M. & Jenkins, M.K. *In situ* analysis reveals physical interactions between CD11b+ dendritic cells and antigen-specific CD4+ T cells after subcutaneous injection of antigen. *J. Immunol.* **169**, 2247–2252 (2002).
5. Negulescu, P.A., Krasieva, T.B., Khan, A., Kerschbaum, H.H. & Cahalan, M.D. Polarity of T cell shape, motility, and sensitivity to antigen. *Immunity* **4**, 421–430 (1996).
6. Dustin, M.L., Bromley, S.K., Kan, Z., Peterson, D.A. & Unanue, E.R. Antigen receptor engagement delivers a stop signal to migrating T lymphocytes. *Proc. Natl. Acad. Sci. USA* **94**, 3909–3913 (1997).
7. Monks, C.R., Freiberg, B.A., Kupfer, H., Sciaky, N. & Kupfer, A. Three-dimensional segregation of supramolecular activation clusters in T cells. *Nature* **395**, 82–86 (1998).
8. Wulfing, C. & Davis, M.M. A receptor/cytoskeletal movement triggered by costimulation during T cell activation. *Science* **282**, 2266–2269 (1998).
9. Grakoui, A. *et al.* The immunological synapse: a molecular machine controlling T cell activation. *Science* **285**, 221–227 (1999).
10. Underhill, D.M., Bassetti, M., Rudensky, A. & Aderem, A. Dynamic interactions of macrophages with T cells during antigen presentation. *J. Exp. Med.* **190**, 1909–1914 (1999).
11. Gunzer, M. *et al.* Antigen presentation in extracellular matrix: interactions of T cells with dendritic cells are dynamic, short lived, and sequential. *Immunity* **13**, 323–332 (2000).
12. Bousso, P., Bhakta, N.R., Lewis, R.B. & Robey, E. Dynamics of thymocyte–stromal cell interactions visualized by two-photon microscopy. *Science* **296**, 1876–1880 (2002).
13. Miller, M.J., Wei, S.H., Parker, I. & Cahalan, M.D. Two-photon imaging of lymphocyte motility and antigen response in intact lymph node. *Science* **296**, 1869–1873 (2002).
14. Stoll, S., Delon, J., Brotz, T.M. & Germain, R.N. Dynamic imaging of T cell–dendritic cell interactions in lymph nodes. *Science* **296**, 1873–1876 (2002).
15. Porgador, A. *et al.* Predominant role for directly transfected dendritic cells in antigen presentation to CD8+ T cells after gene gun immunization. *J. Exp. Med.* **188**, 1075–1082 (1998).
16. Cumberbatch, M., Dearman, R.J. & Kimber, I. Influence of ageing on Langerhans cell migration in mice: identification of a putative deficiency of epidermal interleukin-1β. *Immunology* **105**, 466–477 (2002).
17. Pircher, H., Burki, K., Lang, R., Hengartner, H. & Zinkernagel, R.M. Tolerance induction in double specific T-cell receptor transgenic mice varies with antigen. *Nature* **342**, 559–561 (1989).
18. Miller, M.J., Wei, S.H., Cahalan, M.D. & Parker, I. Autonomous T cell trafficking examined *in vivo* with intravital two-photon microscopy. *Proc. Natl. Acad. Sci. USA* **100**, 2506–2509 (2003).
19. Grufman, P., Wolpert, E.Z., Sandberg, J.K. & Karre, K. T cell competition for the antigen-presenting cell as a model for immunodominance in the cytotoxic T lymphocyte response against minor histocompatibility antigens. *Eur. J. Immunol.* **29**, 2197–2204 (1999).
20. Kedl, R.M. *et al.* T cells compete for access to antigen-bearing antigen-presenting cells. *J. Exp. Med.* **192**, 1105–1113 (2000).
21. Savage, P.A., Boniface, J.J. & Davis, M.M. A kinetic basis for T cell receptor repertoire selection during an immune response. *Immunity* **10**, 485–492 (1999).
22. Busch, D.H. & Pamer, E.G. T cell affinity maturation by selective expansion during infection. *J. Exp. Med.* **189**, 701–710 (1999).
23. Rees, W. *et al.* An inverse relationship between T cell receptor affinity and antigen dose during CD4+ T cell responses *in vivo* and *in vitro*. *Proc. Natl. Acad. Sci. USA* **96**, 9781–9786 (1999).
24. Kedl, R.M., Schaefer, B.C., Kappler, J.W. & Marrack, P. T cells down-modulate peptide-MHC complexes on APCs *in vivo*. *Nat. Immunol.* **3**, 27–32 (2002).
25. Shortman, K. & Liu, Y.J. Mouse and human dendritic cell subtypes. *Nat. Rev. Immunol.* **3**, 151–161 (2002).
26. Reichert, P., Reinhardt, R.L., Ingulli, E. & Jenkins, M.K. Cutting edge: *in vivo* identification of TCR redistribution and polarized IL-2 production by naive CD4+ T cells. *J. Immunol.* **166**, 4278–4281 (2001).
27. McGavern, D.B., Christen, U. & Oldstone, M.B. Molecular anatomy of antigen-specific CD8+ T cell engagement and synapse formation *in vivo*. *Nat. Immunol.* **3**, 918–925 (2002).

© 2003 Nature Publishing Group http://www.nature.com/natureimmunology